Journal of Science and Technology – Engineering and Technology for Sustainable Development
Volume 36, Issue 1, March 2026, 056-067

Study on Photocatalytic and Antibacterial Activity of Ag Doped ZnO Attached on Cotton Fabrics and Evaluation of Antibacterial Durability after Washing Cycles

Phuong Linh Nguyen [1,2], Duy Nam Phan [1,*], Minh Thang Le[1]
[1]*Hanoi University of Science and Technology, Ha Noi, Vietnam*
[2]*Hanoi Industrial Textile Garment University, Ha Noi, Vietnam*
[*]*Corresponding author email: nam.phanduy@hust.edu.vn*

Abstract

The study used the co-precipitation method to synthesize silver (Ag) doped ZnO nanoparticles with different doping contents of 0.5%, 1%, 2%, and 3% (mole fraction). The obtained material properties were tested using methods such as energy dispersive X-ray spectroscopy (EDS), Fourier transform infrared spectroscopy (FTIR), and scanning electron microscopy (SEM). The photocatalytic activity of these materials was assessed by degrading methylene blue (MB) using UV-Vis absorption spectra under ultraviolet, xenon, and sunlight. The antibacterial activity was evaluated using the Kirby-Bauer disc diffusion method against the gram-positive Staphylococcus aureus and gram-negative Escherichia coli bacteria. The results demonstrate that Ag-doped ZnO nanoparticles exhibit a significant increase in photocatalytic performance and antibacterial activity over the undoped ZnO nanoparticles. The sol-gel coating technique was used to attach Ag-doped ZnO nanomaterials to enhance some unique properties of cotton fabrics, such as antibacterial and photocatalytic properties. The ASTM D4265 (Evaluating Stain Removal Performance in Home Laundering) standard was used to evaluate the effectiveness of the coating after washing cycles. Analyzing the adhesion ability of the coating based on SEM, EDS, and FTIR, the ASTM E2149 standard is used to evaluate the antibacterial efficacy of the material.

Keywords: Ag doped ZnO nanoparticles, antibacterial, cotton fabric, sol - gel method, self-cleaning properties.

1. Introduction

Nowadays, the development of semiconductor materials has led to numerous important applications in various fields, such as industry, sensors, cosmetics, the environment, and biomedicine [1]. Nanomaterials such as zinc oxide (ZnO) nanoparticles stand out due to their two significant properties: photocatalysis and antibacterial activity [2]. The ability to absorb light and generate highly oxidative free radicals of ZnO nanoparticles are applied in environmental pollution treatment and decompose of harmful organic substances. Additionally, the mechanism of releasing metal ions and disrupting bacterial cell membranes, these materials are also used for antibacterial products, contributing to improved quality of life and human health protection.

ZnO is one of the important semiconductors. The structure of ZnO is composed of two elements: Zn from group IIB and O from group VIA. ZnO is a wide-bandgap semiconductor belonging to the II-VI semiconductor group, with a hardness of approximately 4.5 on the Mohs scale. It exhibits high thermal, mechanical, and chemical stability, a broad radiation absorption range, and excellent photostability. Zinc oxide is a white, odorless solid with a molecular weight of 81.4 g/mol, a density of 5.6 g/cm³, and a melting point of 2360 ℃. ZnO exists in three structural forms: hexagonal wurtzite, zincblende, and rocksalt, Fig. 1 [3].

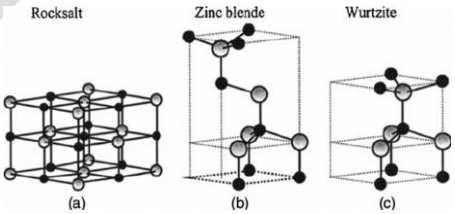

Fig. 1. ZnO crystal structures: simple cubic NaCl-type lattice (a), cubic zinc blende-type lattice (b), and hexagonal wurtzite lattice (c) [3]

ZnO nanoparticles possess a bandgap of about 3.37 eV and a high exciton binding energy of 60 meV [4], allowing strong UV absorption from 200–400 nm. At room temperature, ZnO shows two main photoluminescence regions: near-UV emission around 380 nm, related to electron-hole recombination within the bandgap (a direct-bandgap feature), and visible emission from 400–600 nm, primarily caused by crystal lattice defects. These defects include oxygen vacancies (V_O), interstitial oxygen (O_i), interstitial zinc (Zn_i), and zinc vacancies (V_Zn), which create intermediate energy levels affecting ZnO's luminescence, Fig. 2 [5].

p-ISSN 3093-3242
e-ISSN 3093-3579
https://doi.org/10.51316/jst.188.etsd.2026.36.1.8
Received: Apr 9, 2025; revised: Apr 29, 2025
Accepted: May 26, 2025; Online: Feb 5, 2026.

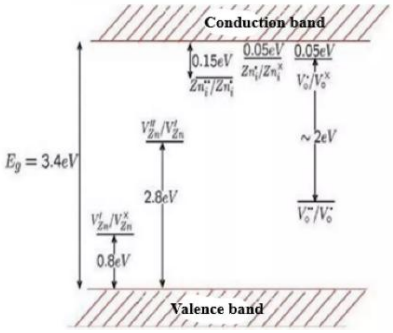

Fig. 2. Calculated defect levels in ZnO nanostructures

When defects form, they create defect energy levels within the bandgap of ZnO.

Oxygen Vacancy (V_O)

Oxygen vacancies are common defects in ZnO, forming energy levels about 2eV below the conduction band. They lower the excitation energy for electrons, leading to green emission and affecting ZnO's photoluminescence efficiency and photocatalytic properties.

Interstitial Zinc Atom (Zn_i)

An interstitial zinc atom occurs when a zinc atom occupies a position outside its standard crystal lattice site. This generates energy levels at 0.15 eV and 0.05 eV below the conduction band. It increases the density of free charge carriers, making ZnO a stronger n-type semiconductor.

Zinc Vacancy (V_Zn)

A zinc vacancy creates a deeper energy level, approximately 2.8 eV below the conduction band. This defect acts as an electron trap, which can reduce the electrical conductivity of ZnO.

In addition, the analysis of point defects in the ZnO crystal includes, Fig. 3 [6, 7].

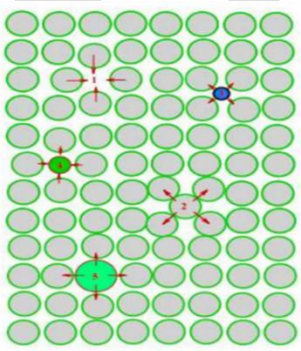

(1) Vacancy

(2) Self-interstitial

(3) Interstitial impurity

(4), (5) Substitutional impurity

Fig. 3. The image shows the defect points of various types in the ZnO structure.

Vacancy (V). Atom missing from the lattice. In ZnO, oxygen vacancies (V_O) and zinc vacancies (V_Zn) act as electron traps, affecting optical and electronic properties.

Self-interstitial (I). Zn or O atoms occupy non-standard positions, altering electrical conductivity by serving as charge centers.

Interstitial impurity (I'). Foreign atoms at interstitial sites modify ZnO's conductivity, optical, or catalytic properties.

Substitutional impurity (S). Foreign atoms replace Zn or O, changing the bandgap and affecting electrical, optical, and photocatalytic properties.

Doping impurities into ZnO nanoparticles compensates for structural defects and optimizes optical, electrical, and photocatalytic properties by controlling charge carrier concentration, modifying the bandgap, and enhancing application performance.

Doping to Control Electrical Properties

ZnO is naturally an *n*-type semiconductor due to oxygen vacancies (V_O) and interstitial zinc atoms (Zn_i), which generate free electrons. Doping with group III elements (Al, Ga, In) further increases *n*-type conductivity. To achieve *p*-type ZnO, doping with group I (Li, Na, K) or group V (N, P, As) elements introduces hole carriers, enabling applications in devices like LEDs and FETs [8].

Doping to Modify Optical Properties

Oxygen vacancies (V_O) create intermediate energy levels in ZnO, causing green emission. Doping with transition metals (Mn, Co, Ni, Cu) introduces specific energy levels, enabling controlled emission at desired wavelengths and expanding ZnO's applications in optoelectronics, sensors, and photocatalysis [8].

Doping to Enhance Photocatalytic Activity

ZnO is an effective photocatalyst but mainly absorbs UV light (200–400 nm). Doping with elements like Fe, Ag, Au, Cu, N, and S creates intermediate energy levels, extending absorption into the visible range (400–700 nm) and improving ZnO's efficiency in pollutant degradation for water and air purification.

Doping to Improve Antibacterial Properties

ZnO exhibits antibacterial activity through Zn^{2+} ion release and radical generation (•OH, O_2^-). Doping with metals like Ag, Cu, and Ti enhances this effect, as Ag^+ and Cu^{2+} ions disrupt bacterial membranes, making ZnO effective for antibacterial fabrics, coatings, and biomedical materials.

Doping is essential for compensating structural defects and optimizing ZnO's electrical, optical, and catalytic properties across applications such as photocatalysis, sensors, LEDs, and environmental treatment.

This article focuses on doping Ag into ZnO nanostructures to significantly enhance both photocatalytic and antibacterial performance, expanding ZnO's potential in environmental and biomedical fields [9].

Enhancement of Photocatalytic Performance

Silver doping helps overcome ZnO's limitations by enhancing visible-light absorption and reducing electron-hole recombination. Through localized surface plasmon resonance (LSPR), Ag extends ZnO's photocatalytic activity into the visible range (400–700 nm). Ag nanoparticles also act as electron traps, improving charge separation and boosting reactive oxygen species (ROS) generation for pollutant degradation in water and air purification.

Improvement of Antibacterial Properties

ZnO intrinsically exhibits antibacterial activity by generating oxidizing radicals (•OH, O_2^-) and releasing Zn^{2+} ions. Ag doping enhances this effect by disrupting bacterial membranes through Ag^+ ions, synergizing with ZnO's ROS generation, and providing prolonged antibacterial action. Ag/ZnO nanocomposites are thus highly effective for antimicrobial coatings, medical devices, wound dressings, and hygiene materials [10].

The incorporation of Ag into ZnO nanostructures provides a dual-function enhancement, significantly improving both photocatalytic activity for environmental applications and antibacterial performance for biomedical and hygienic uses. This doping strategy offers a cost-effective, efficient, and scalable approach to developing high-performance ZnO-based nanomaterials with broad applications in water purification, air treatment, antibacterial textiles, and biomedical coatings.

2. Experimental

2.1. Synthesis of Ag-Doped ZnO Nanoparticles by Co-Precipitation Method

There are various methods for synthesizing ZnO nanoparticles, such as sol-gel, hydrothermal, microwave-assisted, and co-precipitation techniques. Among them, the co-precipitation method is often preferred in laboratory-scale research due to its advantages: simple implementation without complex equipment, low cost with readily available materials, effective control over particle size and morphology through adjustable parameters, high product yield, and environmental friendliness. Compared to hydrothermal and sol-gel methods, co-precipitation offers greater flexibility and is more suitable for early-stage research. Specifically, in the synthesis of Ag-doped ZnO nanoparticles, this method enables precise control of Ag incorporation, ensuring uniform doping while maintaining a simple and cost-effective process.

2.1.3. Chemicals and equipment

The materials and equipment used in the experiment included zinc acetate dihydrate ($Zn(CH_3COO)_2{\cdot}2H_2O$), silver nitrate ($AgNO_3$), potassium hydroxide (KOH), distilled water, ethanol, a magnetic stirrer, a centrifuge machine, a drying oven, a muffle furnace, and filter paper. The chemicals were purchased from Yuanye Biotechnology Co., Ltd., Shanghai, with a purity greater than 96%. The equipment and the synthesis process of ZnO nanoparticles were conducted at the Vietnam-Germany Catalysis Research Center (D8), Hanoi University of Science and Technology.

Ag-doped ZnO nanoparticles were prepared at a doping concentration of 0.5, 1, 2, and 3 % by precipitation method, as in the following steps.

Step 1: Dissolving Zinc Acetate

Weigh an appropriate amount of zinc acetate dihydrate ($Zn(CH_3COO)_2{\cdot}2H_2O$) and completely dissolve it in 50 mL of distilled water to prepare a 0.2M $Zn(CH_3COO)_2{\cdot}2H_2O$ solution. Stir the solution using a magnetic stirrer for 15–30 minutes to ensure complete dissolution of zinc acetate. Add $AgNO_3$ in a corresponding molar ratio to the 0.2M $Zn(CH_3COO)_2{\cdot}2H_2O$ solution. Continue stirring for 30 minutes to achieve a homogeneous solution.

$$Zn(CH_3COO)_2{\cdot}2H_2O \rightarrow Zn^{2+} + 2CH_3COO^- + 2H_2O$$

$$AgNO_3 \rightarrow Ag^+ + NO_3^-$$

Step 2: Precipitation of $Zn(OH)_2$ and Ag(OH)

0.2M KOH solution is added dropwise to the $Zn(CH_3COO)_2$-$AgNO_3$ solution while stirring continuously. The addition and stirring process lasts for 4 hours to ensure uniform precipitation of $Zn(OH)_2$. The pH of the solution is monitored to ensure complete $Zn(OH)_2$ precipitation. (In this experiment, the pH was adjusted to 12 to control the size of the synthesized Ag-doped ZnO nanoparticles).

$$Zn^{2+} + 2OH^- \rightarrow Zn(OH)_2\downarrow$$

$$Ag^+ + OH^- \rightarrow AgOH\downarrow$$

(AgOH is unstable and can easily be reduced to metallic Ag.)

Step 3: Filtration and Purification of the Precipitate

After the reaction is complete, the precipitate is filtered using filter paper or centrifugation. The precipitate is washed multiple times with distilled water to remove excess ions. The purity of the precipitate can be checked using conductivity measurements or spectroscopy.

Step 4: Stabilizing the Precipitate in Ethanol

The precipitate obtained is dispersed in absolute ethanol for about 2 hours to stabilize its structure and control the nanoparticle size.

Step 5: Drying and Calcination of the Precipitate

The precipitate is dried at 75 °C for 6 hours to remove residual solvents. The dried product is then calcined at 450 °C for 3 hours to obtain crystalline Ag-doped ZnO nanoparticles. Finally, the product is calcined again at 450 °C for 3 hours to achieve crystalline Ag-doped ZnO nanoparticles.

$Zn(OH)_2 \rightarrow (\Delta T)\ ZnO + H2O$

Silver hydroxide (AgOH) may undergo reduction to metallic silver (Ag) or silver oxide (Ag_2O) through the following reactions:

$2AgOH \rightarrow (\Delta T)\ Ag_2O + H_2O_2$

$Ag_2O \rightarrow (\Delta T)\ 2Ag + ½\ O_2$

Formation of Ag-Doped ZnO Nanoparticles

Silver (Ag) is either incorporated into the ZnO structure or exists as Ag nanoparticles on the ZnO surface, forming Ag-doped ZnO with enhanced photocatalytic and antibacterial properties.

Overall Reaction:

$Zn(CH_3COO)_2 \cdot + 2KOH + AgNO_3 \rightarrow \Delta T\ ZnO{:}Ag + CH_3COOK + KNO_3 + H_2O$

2.2. Morphological Examination and Catalytic Characterization of Zinc Oxide Nanoparticles

2.2.1. Morphology and catalytic properties of silver doped Zinc Oxide nanoparticles

The properties of nanostructures are highly dependent on their size and shape. The catalytic characterization is performed based on the following analyses: Scanning Electron Microscopy (SEM), Fourier Transform Infrared Spectroscopy (FTIR), Energy Dispersive Spectroscopy (EDS), X-ray Diffraction (XRD), Bandgap Energy Determination (UV-Vis DRS - Diffuse Reflectance Spectroscopy).

2.2.2. Investigation of adsorption and dye degradation ability of Ag-doped ZnO nanocatalysts

Principle of UV-Vis Measurement.

Ultraviolet-Visible Spectroscopy (UV-Vis spectroscopy) is based on the absorption of light by a solution within the ultraviolet (UV, 200–400 nm) and visible (Vis, 400–800 nm) wavelength ranges. When the dye-containing solution undergoes degradation under the catalytic effect of ZnO, the absorbance intensity at the dye's characteristic wavelength gradually decreases over time.

Experimental Procedure.

Step 1: Experimental Preparation

Methylene Blue (MB) dye is used for the reaction. Prepare 100 mL of MB solution with an initial concentration of 10 ppm. Dissolve 0.2 g of Ag doped ZnO catalyst into the solution, ensuring an optimal reaction condition within a pH range of 7–9. The degradation reaction chamber consists of a sealed dark box lined with aluminum foil inside to maintain darkness while preparing samples and to prevent UV radiation leakage. The UV light source is a 60W ultraviolet (UV-C) lamp emitting radiation at 254 nm, positioned 15 cm above the solution's surface to provide photons for the photocatalytic process.

Step 2: Experimental Procedure

Adsorption Process: The MB dye solution and ZnO catalyst mixture is stirred in the dark for 60 minutes to determine the adsorption capacity of the catalyst.

Photocatalytic Degradation: The solution is exposed to UV light, visible light, and sunlight, and the decrease in absorbance intensity is measured over time.

Step 3: UV-Vis Measurement Over Time

Sample Collection: Take 1 mL of the solution at different time intervals (t = 0, 30, 60 minutes, etc.). Centrifuge the samples to separate the catalyst from the solution.

UV-Vis Spectroscopy Measurement: Use a Shimadzu UV-1800 UV-Vis spectrophotometer to measure the absorption spectrum of the solution at each time interval. Monitor changes in absorbance intensity at the dye's characteristic peak wavelength (λ_max).

Data Analysis: All experiments are conducted under the same conditions at room temperature. The solar irradiation pattern was monitored during August 2024 from 10:00 a.m. to 3:00 p.m. Except for sunlight intensity, all other parameters remained constant throughout the experiment.

The degradation of methylene blue is evaluated by integrating the area under the absorbance curve.

A graph of the absorbance ratio (A_t/A_0) vs. time is plotted (A_t: absorbance at time t, A_0: initial absorbance). The photocatalytic degradation efficiency is calculated using the following formula:

$$\text{Degradation Efficiency}(\%) = \left(\frac{A_0 - A_t}{A_0}\right) \times 100 \quad (1)$$

2.3. Process of Coating Cotton Fabric with Pre-Synthesized Ag-Doped ZnO Nanoparticles Using the Sol-Gel Method with Polyvinyl Alcohol as a Binding Agent

The sol-gel method is a widely used technique for coating textiles with nanoparticles, offering advantages such as uniform deposition, strong adhesion, and enhanced functional properties. Ag-doped ZnO nanoparticles (pre-synthesized) can be effectively deposited onto cotton fabric using polyvinyl alcohol (PVA) as a binding agent, which enhances adhesion while maintaining the antimicrobial, UV-blocking, and photocatalytic properties of the nanoparticles.

2.3.1. Chemicals and equipment

The materials used included pre-synthesized Ag-doped ZnO nanoparticles (Ag-ZnO) as the functionalizing agent, PVA (1–5 wt%) as the binder and stabilizer, ethanol and distilled water as solvents, and cotton fabric as the coating substrate.

The equipment comprised a magnetic stirrer and hot plate for sol preparation, an ultrasonic bath for nanoparticle dispersion, a dip-coating apparatus for fabric coating, a drying oven (70–100 °C), a curing furnace (150–200 °C), a pH meter for sol stability control, and a UV-Vis spectrophotometer for optical analysis. Structural and morphological characterization was performed using Scanning Electron Microscopy combined with SEM-EDS and FTIR techniques.

2.3.2. Experimental procedure

Step 1. Preparation of the Ag-ZnO/PVA Sol

Dissolve 3 wt% PVA in 50 mL of distilled water under stirring at 80 °C until a clear solution forms. Then, add 1 wt% pre-synthesized Ag-doped ZnO nanoparticles and disperse them uniformly using an ultrasonic bath for 30 minutes.

$$[CH_2CH(OCOCH_3)]_n + nH_2O \rightarrow [CH_2CH(OH)]_n + nCH_3COOH$$

This forms polyvinyl alcohol (PVA) from polyvinyl acetate (PVAc).

Hydrogen Bonding Between PVA and Ag-ZnO

When Ag-ZnO nanoparticles are introduced into aqueous PVA, they interact via hydrogen bonding:

$$\text{Ag-ZnO} + \text{PVA} \leftrightarrow \text{PVA-ZnO complex}$$

$$\text{Ag-ZnO (nanoparticles)} + \text{PVA} \rightarrow \text{(stirring/ultrasonication) Stable dispersion}$$

Step 2. Coating Cotton Fabric Using Dip-Coating Method

Pre-treat the cotton fabric by washing with distilled water and ethanol, then dry at 70 °C for 1 hour. For dip-coating, immerse the pre-treated fabric in the Ag-ZnO/PVA sol for 5–10 minutes, drain excess sol, and repeat the process 2–3 times for uniform deposition. Finally, dry the coated fabric at 70–100 °C for 2 hours to remove moisture and enhance adhesion.

The cotton fabric is immersed in the Ag-ZnO/PVA sol. The interaction between PVA, ZnO, and cellulose fibers in cotton occurs via hydrogen bonding and Van der Waals forces:

Cotton (Cell-OH) + PVA-ZnO → Cotton-PVA-ZnO Complex

Step 3. Thermal Curing of the Coated Fabric

Cure the coated fabric at 150–200 °C for 2 hours to enhance nanoparticle adhesion, Improve coating durability. Remove residual PVA without damaging the fabric.

If PVA is partially removed to enhance direct ZnO adhesion, it decomposes via:

$$\text{PVA} \rightarrow (\Delta T)\ CO_2 + H_2O + \text{residual carbon}$$

Formation of final Ag-ZnO-Coated Cotton Fabric, the remaining Ag-ZnO nanoparticles bind to the fabric via van der Waals forces, hydrogen bonding, and physical adsorption:

Cotton-OH + Ag-ZnO → (ΔT) Ag-ZnO/Cotton Composite

2.4. Testing the Coating Quality, Photocatalytic and Antibacterial Properties of Cotton Fabric Coated with Ag-Doped Zinc Oxide Nanoparticles

2.4.1. Structural and surface analysis

SEM-EDS was used to determine the surface morphology and the distribution of nanoparticles on the fabric. FTIR was employed to confirm the presence of ZnO, Ag, and their interactions with PVA.

2.4.2. Functional testing

Antibacterial testing was conducted to evaluate the bacterial inhibition efficiency against E. coli and S. aureus following the ASTM E2149 standard. Durability testing was performed to assess the wash resistance of the coating after multiple laundering cycles according to the AATCC 61 standard.

Washing Durability Test of Cotton Fabric Coated with ZnO Nanoparticles

To evaluate the durability of the Ag-doped (ZnO) nanoparticle coating on cotton fabric and assess its photocatalytic and antibacterial effectiveness after multiple washing cycles, the coated fabric samples were washed for up to 20 cycles following the AATCC 61-2013 (2A) standard. After specific washing cycles, the photocatalytic activity was tested by measuring the degradation of methylene blue (MB) solution using UV-Vis spectroscopy, while the antibacterial activity was assessed according to the ASTM E2149-10 standard.

The test sample consisted of cotton fabric coated with ZnO nanoparticles, sized 5 × 10 cm. A multi-fiber cotton fabric was used as the accompanying test fabric. The washing procedure utilized AATCC 1993 WOB standard detergent at a concentration of 0.15 g/L. Washing was conducted at a temperature of 49 °C for 45 minutes, using 100 mL of solution and 10 steel balls to simulate mechanical action during laundering. The washing experiments were conducted using a laundering fastness testing machine at the Laboratory of Textile Materials and Chemical Technology, Institute of Textiles, Leather, and Fashion, Hanoi University of Science and Technology.

Antibacterial Testing of Cotton Fabric Coated with Ag doped ZnO Nanoparticles

The antibacterial effectiveness of Ag-doped ZnO nanoparticle-coated cotton fabric is evaluated following the ASTM E2149 standard, which measures antibacterial activity in actively antimicrobial materials using suspended bacteria (E. coli, S. aureus) and assesses bacterial reduction after exposure.

Step 1. Preparation of Fabric Samples

For testing, cut fabric into 2.5 × 2.5 cm pieces. Prepare 3 test samples (Ag-ZnO-coated fabric) and 3 control samples (uncoated fabric). Sterilize all samples at 121 °C for 15 minutes and dry them under sterile conditions.

Step 2. Preparation of Bacterial Suspension

Selected bacterial strains include Escherichia coli ATCC 25922 (Gram-negative) and Staphylococcus aureus ATCC 6538 (Gram-positive). For culturing, incubate bacteria in Brain Heart Infusion Broth (BHI) at 37 °C for 18–24 hours, then dilute with 0.9% NaCl to a concentration of 10^5–10^6 CFU/mL.

Step 3. Antibacterial Testing Procedure

For bacterial exposure, pour 50 mL of bacterial suspension into a sterile Erlenmeyer flask, immerse the fabric sample, and stir gently at 120 rpm at 37 °C for 1 hour. After exposure, extract 1 mL of the solution and perform serial dilutions (1:10) using 0.9% NaCl.

Step 4. Bacterial Quantification

For bacterial plating, pipette 100 µL from each dilution onto Tryptic Soy Agar (TSA) plates and incubate at 37 °C for 24 hours. After incubation, count the colony-forming units (CFU/mL).

Step 5. Calculation of Antibacterial Efficiency

Repeat the ASTM E2149 test at different washing cycles to evaluate the durability of the antibacterial effect. Measure antibacterial effectiveness after 5, 10, 15, 20 wash cycles according to AATCC 61.

3. Results and Discussion

3.1. SEM – ELEMENTAL MAPING – EDS

The Ag doped ZnO catalyst in powder form was analyzed by SEM-EDS on measuring equipment at the Vietnam-Germany Catalyst Center - Hanoi University of Science and Technology with the following results.

The particle size distribution is relatively uniform, though some agglomeration occurs, forming a rough, porous structure, Fig. 4. Measured nanoparticle sizes are: 91.24 nm, 110.8 nm, 25.81 nm, and 54.52 nm, indicating a broad size range (~25–110 nm) due to agglomeration or Ag doping. Ag doping appears as regions with brighter contrast, attributed to silver's higher atomic number. The porous structure suggests a high surface area, advantageous for photocatalysis, antibacterial activity, and sensor applications.

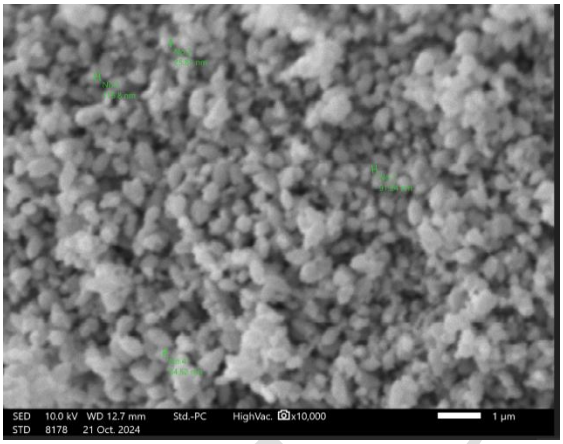

Fig. 4. SEM image of Ag-doped ZnO nanoparticles

The study also synthesized pure zinc oxide nanoparticles using the precipitation method to compare different doping levels.

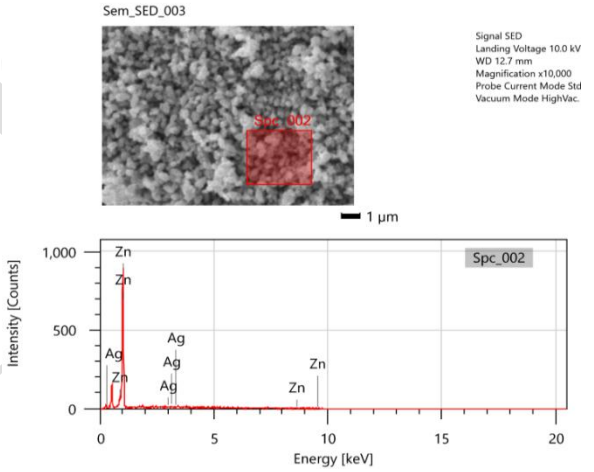

Display name	Standard data	Quantification method	Result Type
Spc_002	Standardless	ZAF	Metal

Element	Line	Mass%	Atom%
Zn	L	99.55±4.10	99.72±4.10
Ag	L	0.45±0.65	0.28±0.39
Total		100.00	100.00
Spc_002			Fitting ratio 0.2140

Fig. 5. EDS analysis of Ag-doped ZnO nanoparticles at 0.5% concentration

Zn is the dominant element (99.72% by mass), indicating that the main structure is composed of ZnO, Fig. 5. Ag is present in a very small quantity (0.45% by mass), which suggests that silver doping is minimal and suitable for doping amount in molar ratio. The atomic percentage of Ag is 0.28%, which is consistent with low-level doping. The standardless quantification method (ZAF correction) was used for composition analysis.

The EDS spectrum shows strong peaks for Zn (Zinc), confirming that ZnO is the primary material. Weak peaks for Ag (Silver) indicate that Ag is successfully incorporated but at low concentrations. No other unexpected elements are detected, suggesting the high purity of the synthesized Ag-doped ZnO.

EDS results with different doping ratios also gave similar elemental compositions indicating the success level in doping Ag with other ratios.

Element	Line	Mass%	Atom%
C	K	7.80±0.45	22.89±1.33
O	K	16.60±0.67	36.58±1.47
Zn	K	74.52±3.66	40.18±1.97
Ag	L	1.08±0.19	0.35±0.06
Total		100.00	100.00
Spc_009			Fitting ratio 0.0394

(a)

Element	Line	Mass%	Atom%
C	K	7.80±0.37	20.77±0.98
O	K	22.78±0.65	45.58±1.29
Zn	K	67.65±2.91	33.12±1.42
Ag	L	1.78±0.20	0.53±0.06
Total		100.00	100.00
Spc_020			Fitting ratio 0.0331

(b)

Fig. 6. EDS analysis of Ag-doped zinc nanoparticles at 1% (a) and 2% (b) concentration

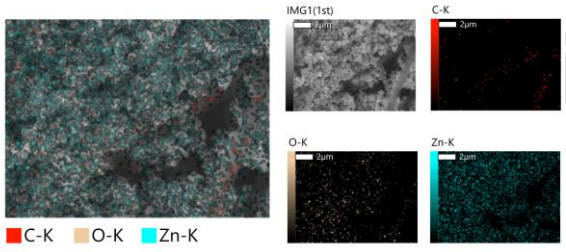

Fig. 7. Elemental Mapping Images of Ag-doped ZnO 0.5%

The structure appears agglomerated and porous, typical of ZnO nanomaterials synthesized by co-precipitation. The variation in contrast may indicate differing elemental distributions or surface topography variations, Fig. 5.

In Fig. 7, very few carbon (C) signals are detected. This suggests that minimal organic contamination is present, indicating good purity of ZnO.The oxygen (O) distribution appears uniformly spread. This confirms the presence of ZnO throughout the mapped area. Oxygen is a key component of ZnO, indicating the successful formation of ZnO nanoparticles.

Zinc (Zn) is highly abundant and uniformly distributed, as seen in the dense green spots. This confirms that the sample is predominantly composed of ZnO nanoparticles.

The image does not show Ag mapping separately, likely because 0.5 mol% Ag is a very low doping concentration, making Ag difficult to detect using standard EDS mapping.

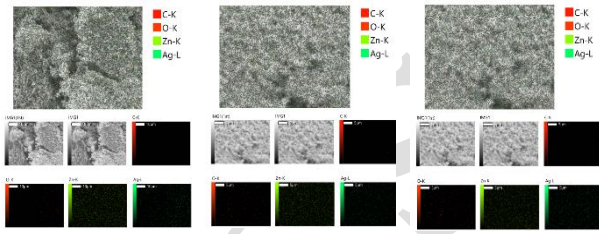

(a) (b) (c)

Fig. 8. Elemental mapping images of Ag-doped ZnO 1%(a); 2% (b); 3% (c) comparison of Ag-doped ZnO nanoparticles (1%, 2%, 3%)

In Fig. 8, at 1% Ag, the Ag distribution appears sparse, with small and widely scattered green points. At 2% Ag, the density of Ag signals increases, showing a more uniform spread. At 3% Ag, the Ag distribution is further enhanced, appearing more densely packed compared to 1% and 2%.

Zn is consistently distributed across all three samples. The intensity of Zn appears similar across the images, indicating that Zn content remains relatively stable regardless of the Ag doping.

Oxygen is more scattered and sparse in all three images. The O intensity remains low and does not significantly change with increasing Ag doping.

Carbon is present in minimal amounts across all images, suggesting that the sample surface is mostly free from contamination.

3.2. Chemical Bond Vibration Analysis (FT-IR)

Analysis and Comparison of Fourier-transform infrared spectroscopy (FT-IR) Spectra of Pure ZnO and Ag-Doped ZnO (0.5%, 1.0%, 2.0%, 3.0%). FT-IR analyzes the chemical bond vibrations in pure ZnO and Ag-doped ZnO at different doping ratios (0.5%, 1.0%, 2.0%, and 3.0%). The spectral analysis helps to identify the functional groups, bond interactions, and changes due to Ag doping.

In Fig. 9 (a), Zn-O stretching vibrations appear in the range of 400–600 cm^{-1}, with peaks around 431 cm^{-1} and 492 cm^{-1}. Weak peaks in the 1500–2000 cm^{-1} range indicate adsorbed water molecules or lattice vibrations. Peaks around 1326 cm^{-1} correspond to C-H bending from possible residual organic compounds. The absence

of strong peaks above 3000 cm^{-1} suggests that there are no significant hydroxyl (-OH) groups.

In all Ag-doped ZnO samples, the Zn-O vibrational bands shift slightly and broaden, which indicates Ag incorporation into the ZnO lattice, Fig. 9 (b), (c), (d), and (e). This broadening is more pronounced in higher Ag doping ratios (1.0%, 2.0%, 3.0%), confirming increased lattice distortion. New peaks in the 2100–2300 cm^{-1} region (C≡C and C≡N stretching vibrations), Peaks in this region appear only in Ag-doped ZnO, suggesting interactions with nitrate precursors or residual organic compounds from synthesis. A broad peak (~3400 cm^{-1}) appears in Ag-doped ZnO, especially at higher Ag concentrations (2.0% and 3.0%). This peak is attributed to hydroxyl (-OH) groups, which indicate an increase in adsorbed water molecules or surface hydroxylation, which is beneficial for photocatalytic activity.

The peaks in the range of 1320 to 1600 cm^{-1} are more pronounced in Ag-doped ZnO, likely due to interactions between Ag and oxygen functional groups.

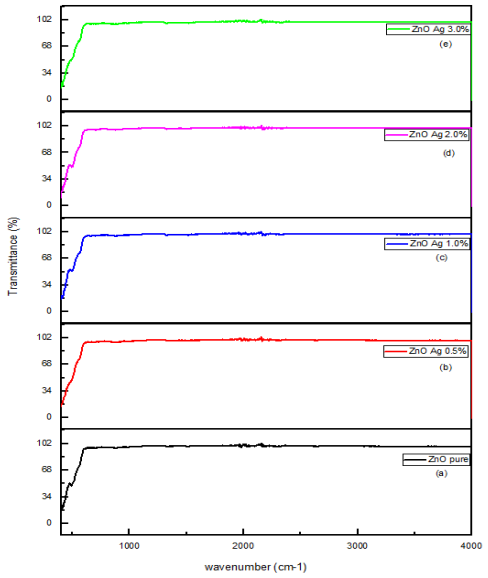

Fig. 9. Chemical bond vibration analysis (FT-IR) of Pure ZnO (a) and Ag-Doped ZnO (0.5% - b, 1.0% - c, 2.0% - d, 3.0% - e) Hydroxyl (-OH) stretching (~3300–3600 cm^{-1})

Zn-O vibrations shift and broaden with increasing Ag doping, confirming successful Ag incorporation into the ZnO lattice. The presence of hydroxyl (-OH) groups increases with Ag content, which may enhance photocatalytic activity. New vibrational peaks (2100–2300 cm^{-1}) appear due to organic residuals or Ag-related interactions. Higher Ag doping (2.0%–3.0%) results in stronger lattice distortions, indicating potential structural modifications. These findings confirm that Ag doping alters the vibrational structure of ZnO, affecting its optical, catalytic, and electronic properties.

3.3. Evaluation of Photocatalytic Ability of Nano Oxide through Methylene Blue Solution Color Decomposition Test

The dye solutions, after undergoing the adsorption process in the dark chamber, were further evaluated for their color concentration transformation with doped ZnO under the influence of Xenon lamp, UV light, and natural light, under continuous stirring conditions. This indicates that the transformation of dye concentration during the decomposition process is independent of the adsorption process. The recorded dye concentration transformation values are presented in Table 1.

Table 1. Decomposition results of MB color of nano zinc oxide, Ag doped zinc oxide under xenon light

Time (minutes)	Eliminate (%) (Xenon)			
	ZnO	Ag-ZnO	Ag-ZnO	Ag-ZnO
0	0.000	0.000	0.000	0.000
30	9.798	9.798	9.798	9.798
60	24.669	41.798	31.124	24.784
90	51.412	66.513	62.305	40.865
120	76.945	92.040	85.280	67.268
150	96.888	99.827	90.127	83.383
180	99.597		98.945	93.078
210			99.867	94.415
240				99.308

The dye degradation under Xenon light were collected and illustrated in the degradation chart, Fig. 10.

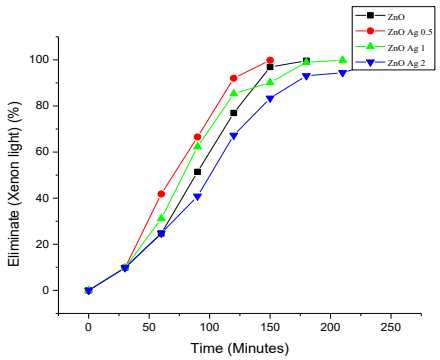

Fig. 10. Decolorization ability of MB solution of ZnO and Ag-doped ZnO under Xenon light

The MB decomposition efficiency increases over time for all samples. The reaction reaches saturation (~100% elimination) after ~200–250 minutes for most catalysts.

Effect of Ag Doping on Photocatalytic Activity:

Ag-doped ZnO (0.5%) shows the highest MB degradation rate, achieving the fastest photocatalytic activity. Ag-doped ZnO (1.0%) also outperforms pure

ZnO but is slightly less effective than 0.5% Ag-ZnO. Pure ZnO exhibits the slowest degradation, confirming the enhancement effect of Ag doping. However, higher Ag doping (2.0%) slightly reduces efficiency, likely due to active site blocking or charge recombination. Low Ag doping (0.5%–1.0%) improves electron-hole separation, reducing recombination and enhancing photocatalytic activity.

At Ag concentrations above 1.0%, Ag nanoparticles may act as recombination centers, reducing charge separation efficiency. Excessive silver also blocks ZnO surface active sites, limiting dye adsorption and photocatalytic performance. Overall, Ag doping enhances ZnO's photocatalytic activity under Xenon light, with 0.5% Ag-doped ZnO showing the best performance, Table 2. Higher doping levels (≥2.0%) decrease efficiency due to recombination and site blocking. Xenon light effectively activates ZnO-based catalysts, supporting their potential for visible-light photocatalysis. 0.5% Ag-doped ZnO is optimal for fast and efficient MB degradation under Xenon light..

Table 2. Comparison of the color decomposition efficiency of MB solution of ZnO and Ag-doped ZnO under Xenon light

Sample	Time to reach ~100% MB Degradation (minutes)	Photocatalytic Efficiency
Pure ZnO	~230–250 min	Lowest
Ag-Doped ZnO(0.5%)	~180–200 min	Highest
Ag-Doped ZnO (1.0%)	~190–210 min	High
Ag-Doped ZnO (2.0%)	~200–220 min	Moderate

The synthesized catalyst demonstrated effective degradation of MB dye under both UV light and sunlight exposure. The results indicate that Ag-doped ZnO with a 0.5% Ag ratio exhibits the highest efficiency in dye degradation during the photocatalytic process, Fig. 11.

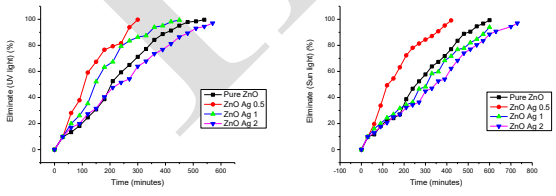

(a) (b)

Fig. 11. Decolorization ability of MB solution of ZnO and Ag-doped ZnO under UV light (a); sunlight (b)

Based on photocatalytic efficiency, 0.5% Ag-doped ZnO nanoparticles are selected for nano-coating cotton fabric using the sol-gel technique with PVA as the binding agent. The coated fabric will undergo durability testing and antibacterial performance evaluation to assess the effectiveness of the Ag-doped ZnO coating.

3.4. Evaluation of Coating Quality and Antibacterial Performance of Ag-Doped ZnO Nanoparticle-Coated Cotton Fabric

In Fig. 12, the surface morphology shows cotton fibers with a wavy structure coated with nanoparticles. Ag-doped ZnO nanoparticles appear as bright spots, distributed relatively uniformly across the fiber surface, although some agglomeration is observed. The ZnO coating is well-adhered to the cotton fibers, with denser clusters in certain areas that could affect the uniformity of functional properties. Overall, Ag-doped ZnO nanoparticles successfully coat the cotton fibers.

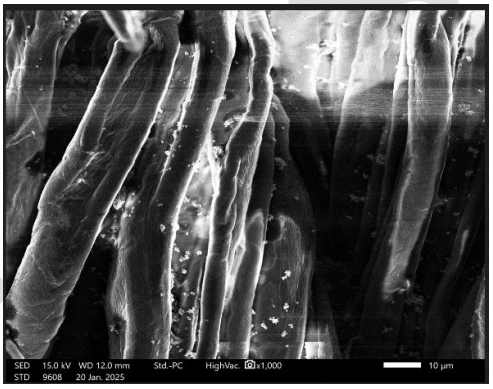

Fig. 12. SEM of Ag-Doped ZnO Nanoparticle-Coated Cotton Fabric

Elemental Mapping

Main SEM Image (Top-Left): Cotton fibers are visible, with nanoparticles attached to the fiber surfaces. The mapping overlay indicates the presence of various elements: C (red), O (orange), Zn (green), and Ag (light green), Fig. 13.

C-K: Present throughout the fibers. Expected, as cotton fabric is cellulose-based (organic).

O-K (Oxygen) (Orange): Spread across the fabric but in discrete points. Likely from the ZnO nanoparticles and cotton's natural oxygen content.

Zn-K (Zinc) (Green): Clearly visible on the fibers, somewhat dispersed. Indicates ZnO nanoparticle deposition but not fully uniform. Some regions appear denser.

Ag-L (Silver) (Light Green): Detected in small clusters across the fabric Confirms the presence of Ag-doped ZnO, though the distribution appears sparse.

Main SEM Image (Top-Left): Cotton fibers are visible, with nanoparticles attached to the fiber surfaces. The mapping overlay indicates the presence of various elements: C (red), O (orange), Zn (green), and Ag (light green).

Zinc Oxide Coating: ZnO is successfully deposited on the cotton fiber surfaces. However, ZnO nanoparticles appear unevenly distributed, suggesting potential aggregation in some regions.

Silver Presence: Ag is detected (light green spots), but the concentration seems low. This aligns with the EDS results, where Ag detection was very low or near the detection limit.

Oxygen Contribution: Oxygen is distributed similarly to Zn, confirming it is part of the ZnO coating rather than just from the cotton fabric.

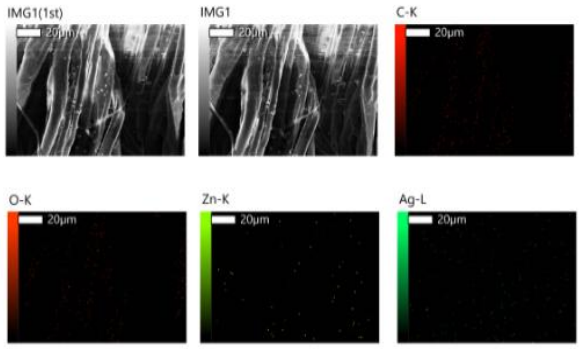

Fig. 13. Elemental Mapping of Ag-Doped ZnO Nanoparticle-Coated Cotton Fabric

FTIR Analysis and Comparison of Uncoated Cotton vs. Ag-Doped ZnO-Coated Cotton Fabric, Fig. 14.

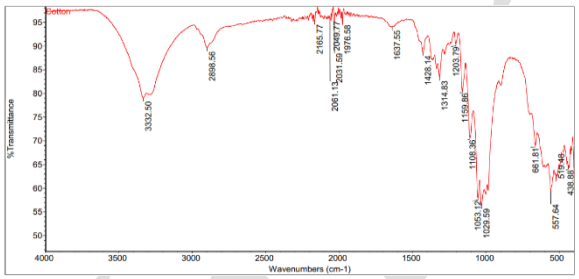

Fig. 14. FTIR Analysis of Cotton

Both spectra exhibit common characteristic peaks related to cotton, which consists mainly of cellulose. The coated fabric spectrum shows additional features due to Ag-doped ZnO nanoparticles, confirming successful coating.

Retention of Cotton's Functional Groups: The major cellulose peaks (O-H, C-H, C-O) remain largely unchanged, indicating that the Ag-doped ZnO coating does not chemically degrade the fabric. New Peaks in Coated Fabric: The Zn-O stretching peaks (~500–700 cm^{-1}) confirm the presence of ZnO nanoparticles. A new peak at ~1730 cm^{-1} (C=O stretch) suggests possible interactions with Ag-doped ZnO or additional organic compounds from the synthesis process. Broadening of O-H Peak (~3330 cm^{-1}): The coated fabric exhibits a broader O-H peak, likely due to ZnO interaction or additional hydrogen bonding effects. So, the FTIR spectra confirm the presence of Ag-doped ZnO nanoparticles on the coated cotton fabric. Zn-O vibration peaks (~500-700 cm^{-1}) are observed only in the coated sample, proving ZnO deposition.

The fabric structure remains intact, with only slight peak shifts and additional signals due to interactions with the coating. The coating method successfully incorporates ZnO without damaging the cellulose structure.

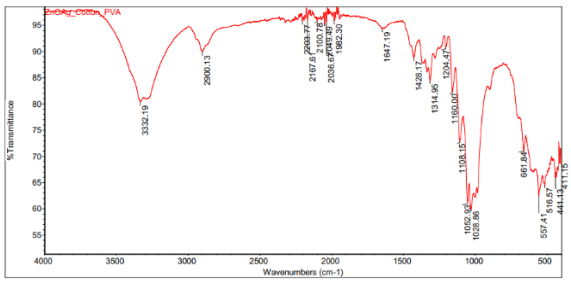

Fig. 15. FTIR Analysis of Ag-Doped ZnO-Coated Cotton Fabric

3.5. Evaluating the effectiveness of a nano oxide coating on cotton fabric

The nano-coated fabric samples were washed for a total of up to 15 washing cycles, following the AATCC 61-2013 (2A) standard. After multiple washing cycles, the fabric samples were analyzed for their morphology using SEM, Elemental Mapping, and EDS. Additionally, their antibacterial properties were evaluated according to the ASTM E2149-10 standard. Testing was conducted after 5, 10, and 20 washing cycles.

In Fig. 16, first image (a- 5 washes) appears to have a more uniform nano-coating with minimal detachment. The second image (b-10 washes) shows some coating loss, with visible fiber exposure and coating fragmentation. The third image (c-20 washes) suggests significant degradation, as many fibers appear more exposed and fragmented.

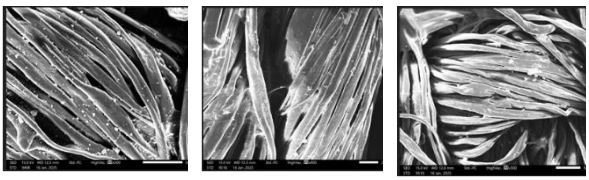

After 5 washes (a) | After 10 washes (b) | After 20 washes (c)

Fig. 16. SEM of Ag-doped ZnO nano-coated cotton fabric after washes

In the initial stage (5 washes), the fibers seem smoother with a more intact structure. By 10 washes, surface roughness increases due to partial coating wear-off. At 20 washes, fibers exhibit cracks, peeling, and detachment of the nano-coating, indicating reduced durability, Fig. 17.

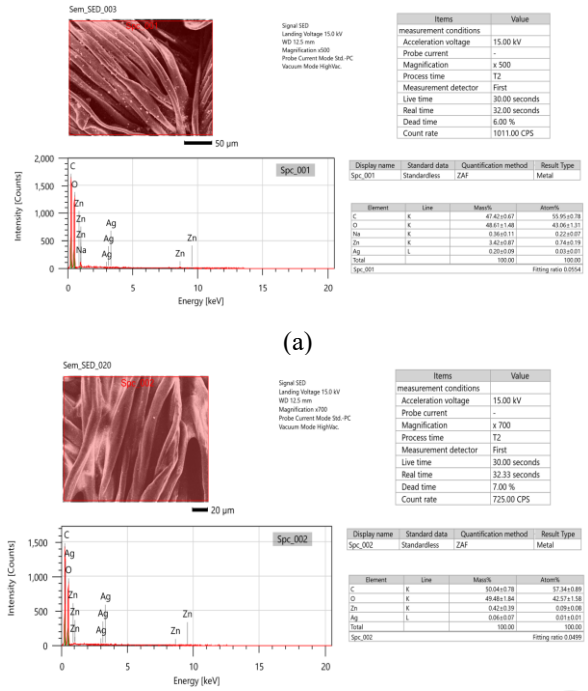

(a)

(b)

Fig. 17. EDS of of nano Ag doped zinc oxide coated on cotton fabric before washing (a) and after 20 washes (b)

The presence of nano-particles is more evident in the 5-wash sample, showing a relatively even spread. By 10 washes, some clustering and voids where coatings have detached become noticeable. At 20 washes, a significant reduction in nano-particles is observed, possibly due to washing-induced erosion. The nano-coating on the fabric degrades progressively with washing, with notable structural and chemical wear after 10 and especially 20 washes.

Based on the elemental analysis from EDS The analysis of the EDS results shows that the ZnO content in the nano-coated fabric decreased from 8.43% (before washing) to 3.18% (after 20 washes). This corresponds to a 62.28% reduction in ZnO content due to washing.

3.6. Antibacterial testing of cotton fabric coated with Ag doped ZnO nanoparticles

Fig. 18 shows photographs of the antibacterial activity on Petri dishes after 24 hours of incubation with fabric samples, before and after washing cycles. The results indicate that all samples maintained strong antibacterial effects against E. coli and S. aureus strains, even after up to 20 washing cycles.

The antibacterial performance evaluation of the fabric samples in Table 3 indicates that the CoAgZnOW0 fabric sample demonstrates strong antibacterial properties against both bacterial strains. Within 1 minute of contact, the bacterial reduction rates reached 94.74% and 92%, and after 1 hour of contact, these rates increased to 99.99%. Fabric samples subjected to 5, 10, and 15 washing cycles maintained 99.99% and 96.73% antibacterial efficiency against E. coli and S. aureus after 1 hour of contact. However, after 20 cycles, a noticeable decline in antibacterial efficiency was observed. This reduction can be attributed to the interaction between AgZnO nanoparticles (AgZnONPs) and the cotton fibers. Initially, the coating solution penetrates deep into the fiber core, becoming embedded within the structure and on the fiber surface, leading to a controlled release mechanism. However, repeated washing gradually degrades the PVA binder, weakening the bond between the nanoparticles and the fabric, making the nano-coating more susceptible to detachment.

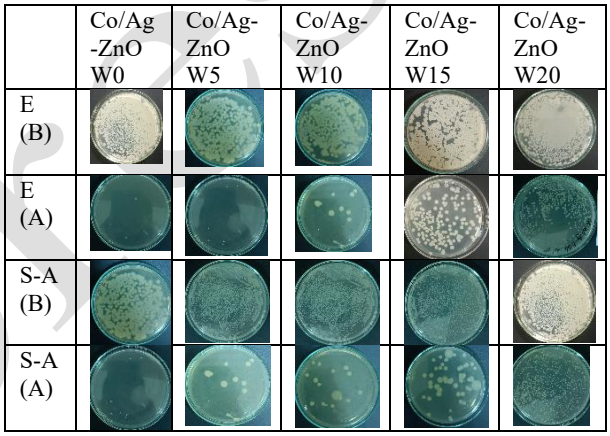

Fig. 18. Results of antibacterial durability assessment of fabrics after washing cycles

As a result, the antibacterial durability remains high (above 90%) for up to 20 washing cycles. Beyond 20 cycles, SEM and EDS analyses show a significant reduction in nanoparticle presence, which correlates with a decrease in antibacterial effectiveness compared to other samples.

4. Conclusion

This study successfully synthesized Ag-doped ZnO nanoparticles using the co-precipitation method. The results demonstrate that Ag-doped ZnO catalysts exhibit high photocatalytic efficiency, effectively degrading MB dye under xenon, UV, and natural light illumination.

The sol-gel coating method enhances the practical applicability of Ag-doped ZnO catalysts. While PVA improved nanoparticle adhesion, it also impacted catalytic activity. Therefore, further improvements and optimization of concentration and coating techniques are necessary to ensure strong adhesion, long-term durability, and enhanced photocatalytic efficiency and antibacterial of the material.

Table 3. Antibacterial Efficiency of CoAgZnO fabrics before and after washing cycles

Sample	Bacterial strain	Initial bacterial density (CFU/ml)	Bacterial density after exposure time (CFU/ml)		Antibacterial efficiency (%)	
			01 minutes	60 minutes	01 minutes	60 minutes
CoAgZnOW0	E. coli (ATCC 8739)	1.9×10^5	1×10^4	0	94.74	99.99
CoAgZnOW5		1.96×10^5	2×10^4	0	89.80	99.99
CoAgZnOW10		2.1×10^5	1.6×10^4	0	92.38	99.99
CoAgZnOW15		2.6×10^5	5.4×10^4	8.5×10^3	79.23	96.73
CoAgZnOW20		1.8×10^5	1.7×10^4	9×10^3	90.56	95.00
CoAgZnOW0	S. aureus (ATCC 2592)	2.5×10^5	2×10^4	0	92.00	99.99
CoAgZnOW5		2×10^5	1.35×10^4	0	93.25	99.99
CoAgZnOW10		3×10^5	2.6×10^4	0	91.33	99.99
CoAgZnOW15		1.8×10^5	3.2×10^4	5.2×10^3	82.22	97.11
CoAgZnOW20		1.5×10^5	6.3×10^4	6.7×10^3	58.00	95.53

Future research will focus on improving Ag-doped ZnO adhesion to fabric, optimizing binder formulations to maintain photocatalytic activity after multiple uses, and enhancing antibacterial durability.

The application of Ag-doped ZnO-based coatings in a sustainable fashion could lead to the production of self-cleaning, antibacterial textiles without the need for harmful chemicals. As the industry shifts towards green technology, improving Ag-doped ZnO immobilization techniques to enhance coating efficiency and durability will be a key focus of future research.

References

[1] Noman, M. T., N. Amor, and M. Petru, Synthesis and applications of ZnO nanostructures (ZONSs): a review. Critical Reviews in Solid State and Materials Sciences, vol. 47, iss. 2, pp. 99–141, 2022. https://doi.org/10.1080/10408436.2021.1886041

[2] Sharma, D. K., Shukla S., Sharma, K. K., and Kumar, V., A review on ZnO: fundamental properties and applications, Materials Today: Proceedings, vol. 49, part 8, pp. 3028–3035, 2022. https://doi.org/10.1016/j.matpr.2020.10.238.

[3] Espitia, P. J. P., Soares, N. F. F., Coimbra, J. S. R., Andrade, N. J., Cruz, R. S., and Medeiros E. A. A., Zinc oxide nanoparticles: synthesis, antimicrobial activity and food packaging applications, Food and Bioprocess Technology, vol. 5, pp. 1447–1464, 2012. https://doi.org/10.1007/s11947-012-0797-6

[4] Nundy, S., Ghosh, A., and Mallick, T. K., Hydrophilic and superhydrophilic self-cleaning coatings by morphologically varying ZnO microstructures for photovoltaic and glazing applications, ACS omega, vol 5, iss. 2, pp. 1033–1039, Jan. 2020. https://doi.org/10.1021/acsomega.9b02758

[5] Fan, J. C., Sreekanth, K. M., Xie, Z., Chang, S. L., Rao, K. V., p-type ZnO materials: theory, growth, properties and devices, Progress in Materials Science, vol. 58, iss. 6, pp. 874–985, Jul. 2013. https://doi.org/10.1016/j.pmatsci.2013.03.002

[6] Sky, T. N., Jahansen, K. M., Riise, H. N., Svensson, B. G., Vines, L., Gallium diffusion in zinc oxide via the paired dopant-vacancy mechanism, Journal of Applied Physics, vol. 123, iss. 5, Feb. 2018. https://doi.org/10.1063/1.5000123.

[7] Yaqoob, F., Ion Implantation in ZnO: defect interaction and impurity diffusion, State University of New York at Albany ProQuest Dissertations and Theses, 2015, pp. 11–24.

[8] K. Omri, A. Bettaibi, K. Khirouni, and L. El Mir, The optoelectronic properties and role of Cu concentration on the structural and electrical properties of Cu doped ZnO nanoparticles, Physica B: Condensed Matter, vol. 537, pp. 167–175, May 2018. https://doi.org/10.1016/j.physb.2018.02.025.

[9] Izunna S. Okeke, Kenneth K. Agwu, Augustine A. Ubachukwu, Fabian I. Ezema, Infuence of transition metal doping on physiochemical and antibacterial properties of ZnO–nanoparticles: a review, Applied Surface Science Advances, vol. 8, Apr. 2022, Art. no. 1000227. https://doi.org/10.1016/j.apsadv.2022.100227

[10] Guan, R., Zhai, H., Sun, D., Zhang, J., Wang, Y., and Li, J., Effects of Ag doping content and dispersion on the photocatalytic and antibacterial properties in ZnO nanoparticles, Chemical Research in Chinese Universities, vol. 35, pp. 271–276, Mar. 2019. https://doi.org/10.1007/s40242-019-8275-6